In Vivo Effect of Selective Macrophage Suppression on the Development of Intrahepatic Cholestasis in Mice

T. A. Korolenko, M. S. Klishevich, M. S. Cherkanova, T. V. Alexeenko, S. Ya. Zhanaeva, N. G. Savchenko, I. A. Goncharova, and E. E. Filjushina

Translated from *Byulleten' Eksperimental'noi Biologii i Meditsiny*, Vol. 146, No. 10, pp. 376-380, October, 2008
Original article submitted February 6, 2008

We studied the role of selective suppression of liver Kupffer cells (gadolinium chloride, 14 mg/kg intravenously) in the development of intrahepatic cholestasis in CBA/C57Bl/6 mice after intraperitoneal injection of α-naphthylisothiocyanate in a single dose of 200 mg/kg. Pretreatment with gadolinium chloride increased the severity of cholestasis and signs of liver damage. Gadolinium accumulation in the liver peaked after 24 h and was accompanied by a decrease in activities of cathepsin D and cathepsin B and concentration of matrix metalloprotease-2. Our results confirm the hypothesis that normal function of Kupffer cells and extracellular matrix plays an important role in cholestasis. Administration of gadolinium chloride serves as a convenient model to study the side effects, toxicity, and safety of lanthanides as nanoparticles.

Key Words: *proteases; α-naphthylisothiocyanate; intrahepatic cholestasis; gadolinium chloride; macrophage suppression*

Biliary obstruction and cholestasis associated with impairment of bile secretion are often observed in patients with chronic liver diseases. Experimental models of cholestasis in laboratory animals allow us to evaluate the pathophysiological and molecular mechanisms of this disorder. Correlations were revealed between experimental disturbances in animals and cholestasis in patients [5,8,12]. Experimental cholestasis in rats and more rarely in mice can be induced by not only common bile duct ligation, but also treatment with estrogens, endotoxins, and various medical products [6,15].

Intrahepatic cholestasis induced by α-naphthylisothiocyanate (ANIT) is a convenient model for studies of hepatocyte injury and compensatory mechanisms in spontaneous recovery of liver function [10,13]. Changes in hepatocyte transport proteins and dysregulation of bile secretion were revealed in mice with experimental cholestasis [8,10]. Cholestasis in mice and rats was observed in the early period after ANIT treatment (4-8 h). The severity of cholestasis depended on the dose of ANIT, route and regimen of treatment, and basal level of cytokines (tumor necrosis factor-α, TNF-α) [11,13,14]. Repeated administration of ANIT to mice is accompanied by the development of biliary cirrhosis; the mechanism of this phenomenon xremains unclear [3-5]. Little is known about the role of Kupffer cells in the development of intrahepatic cholestasis. In the present study, liver macrophage function in mice was suppressed with gadolinium chloride (GC). The role of liver macrophages in the development of cholestasis was evaluated.

GC is used for selective suppression of liver macrophages to study the role of these cells in some disease [1,2]. Intravenous injection of GC to animals is followed by selective elimination of large Kupffer cells [1,9], inhibition of receptor-mediated

Institute of Physiology, Siberian Division of the Russian Academy of Medical Sciences, Novosibirsk, Russia. ***Address for correspondence:*** t.a.korolenko@iph.ma.nsc.ru. T. A. Korolenko

0007-4888/08/1464-0396

endocytosis and phagocytosis of carbon particles [1,2], and increase in the production of proinflammatory cytokines TNF-α and interleukin-6 (IL-6) [2,6,7].

Here we studied the role of liver macrophage suppression in the development of experimental intrahepatic cholestasis in mice.

MATERIALS AND METHODS

Experiments were performed on adult male CBA/C57Bl/6 mice weighing 25.4±1.0 g and obtained from the vivarium of the Institute of Physiology (Siberian Division of the Russian Academy of Medical Sciences) and Institute of Cytology and Genetics (Siberian Division of the Russian Academy of Sciences). Oil solution of ANIT (Aldrich) was injected intraperitoneally in a single dose of 200 mg/kg (n=10-12). The animals were euthanized 24 h after ANIT injection. This compound did not cause death of experimental animals.

GC (Prof. Hardonk, Netherlands) in a single dose of 14 mg/kg was injected into the caudal vein (n=10-12) [1,2]. During combined treatment (n=10-12), GC was administered 24 h before ANIT injection. The animals were euthanized 24 h after ANIT injection. Intact animals served as the control. GC accumulation in the liver was studied after de-ashing of the liver tissue by means of adsorption spectroscopy on a Jober Ivon spectrometer [1].

Activities of alanine transaminase (ALT), aspartate transaminase (AST), and alkaline phosphatase and serum concentration of bilirubin were measured on a Cobas Mira biochemical analyzer (La Roche) with Biocon Diagnostics and Biosystems kits. Total cholesterol concentration in the serum and bile of mice was measured enzymatically with Novokhol kits (Vektor Best). The measurements were performed on a semiautomatic photometer 5010 equipped with a temperature-controlled flow cell (Robert Riele). Triglyceride concentration was measured by the colorimetric method with Triglitseridy-Novo kits (Vektor Best). γ-Glutamyl transpeptidase activity in urine samples was measured in a kinetic study with Biocon Diagnostics kits (activity of this enzyme in the serum was not detected). The measurements were performed on a semiautomatic biochemical photometer equipped with a temperature-controlled flow cell (Screen Master, Hospitex Diagnostics).

Activities of cathepsin B (substrate Z-Arg-Arg-MCA, carbobenzoxy-arginyl-arginine-methylcoumarylamide, NPO Vektor), cathepsin L (substrate Z-Phe-Arg-MCA, carbobenzoxy-phenylalanine-arginine-methylcoumarylamide, NPO Vektor), and cathepsin S (substrate Z-Val-Val-Arg-MCA, carbobenzoxy-valyl-valyl-arginine-methylcoumarylamide, Sigma) were measured fluorometrically [1,15]. The final concentration of a specific cathepsin B inhibitor CA-74 was 10 μM. Fluorescence was measured on a Perkin-Elmer 650-10 S spectrofluorometer at extinction and emission wavelengths of 355 and 460 nm, respectively. The results are expressed in nmol methylcoumarylamide/mg protein/h.

Cathepsin D activity was measured spectrophotometrically. The solution of azocasein (2%, Fluka) in 6 M urea served as the substrate. The concentration of specific cathepsin D inhibitor pepstatin A was 10 μM [15]. Optical density was measured on a Spekol 20 spectrophotometer at 366 nm. The results are expressed in arbitrary laboratory units (U_{366}) per mg protein/h.

Total metalloprotease-2 concentration (MMP-2, gelatinase-2) in blood serum and liver homogenate was estimated by enzyme-linked immunosorbent assay (ELISA) with Quantikine R&D Systems kits for quantitative study of the active enzyme and MMP-2 proenzyme in human/mouse/rat biological samples. The intensity of staining was evaluated on a plate reader (Thermo Electron Corporation Multiscan EX) at 450 nm. The results were calculated from the standard curve and expressed in nanograms MMP-2/ml serum and nanograms MMP-2/g wet tissue. The concentration of tissue inhibitor of metalloproteases-1 (TIMP-1) in blood serum and liver homogenate was measured with commercial EIA kits (Ray Biotech Mouse ELISA Kit) for a quantitative study of TIMP-1 in the serum, plasma, and supernatant of mouse cell cultures. The measurements were performed on a plate reader (Thermo Electron Corporation Multiscan EX) at 450 nm. The results were calculated from the standard curve and expressed in picograms TIMP-1/ml blood serum, picograms TIMP-1/g wet tissue, and picograms TIMP-1/g protein.

Electron microscopy of the liver was performed by the standard method on a JEM-100 SX electron microscope (JEOL). The numerical density of liver macrophages was measured morphometrically.

The results were analyzed by the algorithm of parallel series (variational statistics) with Student's t test. The differences were significant at $p<0.05$. Nonparametric methods of statistical treatment (Mann—Whitney U test) were used when the samples did not conform to normal distribution.

RESULTS

Administration of GC in single doses of 5.0-7.5 mg/kg is followed by selective elimination of large Kup-

ffer cells, but has no effect on functional activity of macrophages in mouse lungs and spleen [1,2]. Increasing the dose of GC to 20 mg/kg is accompanied by severe dysfunction of macrophages not only in the liver, but also in the lungs and intestine [2].

Electron microscopy showed that injection of GC (14 mg/kg) was followed by a significant decrease in the numerical density (788.0±69.1 *vs*. 1053.0±60.5 per mm^2 in the control, $p<0.01$) and size of liver macrophages. The relative volume of primary lysosomes and, particularly, of secondary lysosomes was lower than in the control (1.70±0.64 and 7.60±1.08%, respectively, $p<0.01$).

High concentration of GC in the liver was associated with selective intralysosomal accumulation in nonparenchymal liver cells (85% of the administered dose). Functional state of the liver (serum ALT activity) remained unchanged under these conditions (Table 1). The decrease in the number of liver macrophages and lysosomes in these mice was accompanied by a decrease in specific activity of lysosomal enzymes cathepsin D and cathepsin B in liver homogenates (Table 1). No changes were found in activities of cathepsin S and macrophage-specific cysteine protease. Total MMP-2 concentration (proenzyme and active enzyme) decreased in blood serum. TIMP-1 concentration (major endogenous MMP regulator) remained unchanged in blood serum, but increased in liver homogenates (Table 1). These changes are probably related to interaction between Kupffer cells and stellate cells in the liver, which serve as the main source of MMP and TIMP-1. Our results indicate that single injection of GC is followed by a decrease in activities of lysosomal cysteine and aspartyl proteases. The observed changes are associated with a decrease in the number and functional activity of Kupffer cells. Special attention was paid to a decrease in activity of cathepsin B (probably secretion of extracellular cathepsin B), which serves as a lysosomal cysteine protease in macrophages. Cathepsin B is involved in cascade activation of other proteases that play a role in extracellular matrix degradation and macrophage migration.

Single injection of ANIT was followed by severe ultrastructural changes in liver cells and microcirculatory bed (Fig. 1). They included dilation of sinusoids and intercellular space, widening of bile capillaries (many capillaries of oval shape, Fig. 1), and degeneration of some hepatocytes. Hepatocyte cytoplasm contained numerous lipid inclusions. These signs reflect the development of intrahepatic cholestasis and degeneration of some hepatocytes.

Injection of ANIT to intact mice was followed by an increase in AST activity (287.2±19.0 *vs*. 205.1±7.4 U/liter in the control, $p=0.0001$). The increase in the concentration of total bilirubin (86.2±8.6 *vs*. 9.9±0.8 mmol/liter in the control, $p<0.001$) and conjugated bilirubin (45.6±4.3 *vs*. 6.10±0.39 mmol/liter in the control, $p<0.001$) in blood serum reflects the development of cholestasis in mice. This conclusion was confirmed by a sharp increase in γ-glutamyl transpeptidase activity in urine samples (135.8±30.7 *vs*. 7.2±1.0 U/liter in the control, $p=0.02$). Our results indicate that hepatocyte injury and cholestasis are observed 24 h after ANIT treatment. Total cholesterol concentration increased in blood serum (Fig. 2). Triglyceride level increased, while cholesterol concentration decreased in the bile (Fig. 2). Cholesterol serves as a common precursor of

TABLE 1. Effect of GC on Activities of Cysteine and Aspartyl Proteases in the Liver and Serum Concentrations of MMP-2 and TIMP-1 in Mice

Parameter	Group	
	intact (n=24)	GC, 14 mg/kg, 24 h before ANIT (n=10)
ALT activity in blood serum, U/liter	54.20±1.55	44.6±6.1
Cathepsin B	0.27±0.02	0.20±0.02*
Cathepsin L	0.46±0.03	0.46±0.03
Cathepsin S	0.030±0.002	0.030±0.001
Cathepsin D	0.10±0.08	0.060±0.007$^+$
Total MMP-2 concentration in the serum, ng/ml	201.50±4.66	181.70±4.64$^+$
Serum TIMP-1 concentration, pg/ml	8000.0±1443.4	8450.0±1472.2
TIMP-1 concentration in the liver homogenate, pg/ml	172 143±14 914	224 571±12 750$^+$

Note. Number of animals is shown in brackets. Activities of cathepsin B (substrate Z-Arg-Arg-MCA), cathepsin L (substrate Z-Phe-Arg-MCA), and cathepsin S (substrate Z-Val-Val-Arg-MCA) in liver homogenates are expressed in nmol MCA/mg protein/min. Cathepsin D activity is expressed in U_{366}/mg protein/h. *$p<0.05$ and $^+p\leq0.01$ compared to intact animals.

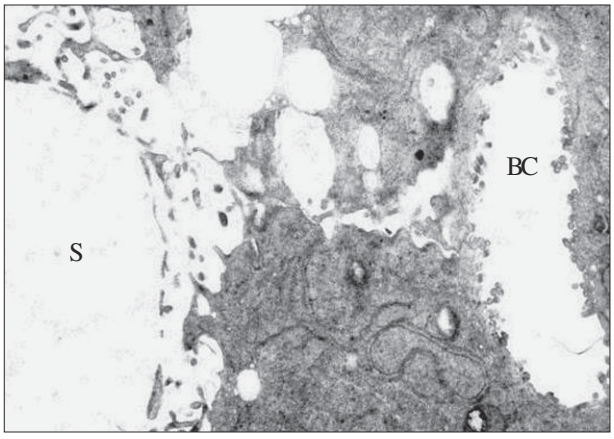

Fig. 1. Electron diffraction pattern of the liver section from mice after single treatment with ANIT. Dilated sinusoid (S) and bile capillary (BC). Large lipid inclusions in hepatocytes, ×16,000.

bile acids. The ANIT-induced increase in serum cholesterol concentration reflects lipid metabolism disorders, which is manifested in lipid infiltration of the liver and cholestasis.

Pretreatment of ANIT-treated animals with GC was followed by an increase in activities of ALT (133.5±37.6 *vs*. 74.70±9.18 U/liter in the ANIT group, p=0.005), alkaline phosphatase (269.1±9.1 *vs*. 158.6±11.1 U/liter in the ANIT group, p=0.0001), and γ-glutamyl transpeptidase in urine samples (243.0±10.0 *vs*. 135.8±30.7 U/liter in the ANIT group, p<0.05). Hence, the severity of cholestasis and hepatocyte injury increased after combined treatment with these compounds. Aggravation of cholestasis under conditions of macrophage suppression in ANIT-treated animals was probably associated with the increased secretion of TNF-α. GC exposure is accompanied by changes in protease

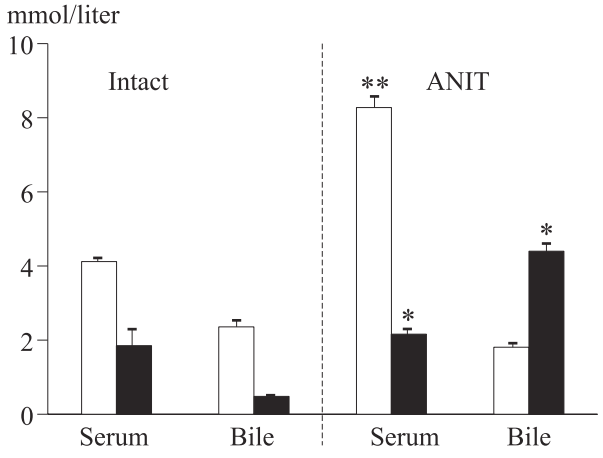

Fig. 2. Total cholesterol concentration and triglyceride level in blood serum and bile from ANIT-treated mice. Light bars, cholesterol; dark bars, triglycerides. *p<0.05 and **p<0.001 compared to intact animals.

secretion from Kupffer cells and stellate cells, remodeling of the extracellular matrix, and repopulation of liver macrophages.

Cholestasis and hyperbilirubinemia in ANIT-treated rats are similar, but more pronounced than the signs observed in patients with cholestasis due to medical treatment (phenothiazine derivatives, methyltestosterone, estrogens, oral contraceptives, *etc*.) [10,14,15]. Hence, this model was used in several experimental studies. It was hypothesized that the development of cholestasis in ANIT-treated rats is associated with direct damage to the bile canaliculi and probably results from parenchymal cell injury and infiltration with polymorphonuclear leukocytes [8,10,11]. Morphological signs of liver cells were similar after ANIT treatment and bile duct ligation [6]. Bile duct cannulation before ANIT administration prevented the development of hyperbilirubinemia and cholestasis. These data indicate that metabolic disorders play an important role after ANIT treatment [10]. Previous studies showed that toxic hydrophobic metabolites of bile acids have surface-active properties and cause hepatocyte membrane injury. Cholestasis is accompanied by severe oxidative stress due to the increased production of lipid peroxides and mitochondrial dysfunction [4,8]. The increase in the production and secretion of proinflammatory cytokines (TNF-α, IL-6, *etc*.) are accompanied by GC-induced variations in proteases. These changes probably contribute to aggravation of cholestasis in ANIT-treated mice. Administration of GC serves as a convenient model of macrophage suppression to study the side effects, toxicity, and safety of lanthanides as nanoparticles. Our results confirm the hypothesis that normal function of Kupffer cells and extracellular matrix plays an important role in cholestasis. Much recent attention is paid to the possibility of treatment with gadolinium compounds during liver transplantation, prevention of anaphylactic shock [2], and immunomodulation in the early stage of sepsis [2,10]. The mechanisms of protective activity of these compounds require further investigations.

We are grateful to V. I. Kaledin (Senior Researcher, Institute of Cytology and Genetics) for his help in this study.

REFERENCES

1. T. A. Korolenko, M. A. Dergunova, T. V. Alexeenko, *et al*., *Byull. Eksp. Biol. Med*., **142**, No. 10, 369-373 (2006).
2. L. C. Adding, G. L. Bannenberg, and L. E. Gustafsson, *Cardiovasc. Drug Rev*., **19**, No. 1, 41-56 (2001).
3. P. K. Baier, U. Baumgartner, S. Hempel, *et al*., *Eur. Surg. Res*., **37**, No. 5, 290-297 (2005).

4. A. Canbay, A. E. Feldstein, H. Higuchi, *et al*., *Hepatology*, **38**, No. 5, 1188-1198 (2003).
5. S. Gehring, E. M. Dickson, M. E. San Martin, *et al*., *Gastroenterology*, **130**, No. 3, 810-822 (2006).
6. J. S. Gujral, J. Liu, A. Farhood, and H. Jaeschke, *Hepatology*, **40**, No. 4, 998-1007 (2004).
7. M. Ide, M. Kuwamura, T. Kotani, *et al*., *J. Comp. Pathol*., **133**, Nos. 2-3, 92-102 (2005).
8. H. Jaeschke, J. S. Gujral, and M. L. Bajt, *Liver Int*., **24**, No. 2, 85-89 (2004).
9. C. Ju, T. P. Reilly, M. Bourdi, *et al*., *Chem. Res. Toxicol*., **15**, No. 12, 1504-1513 (2002).
10. P. Kodali, P. Wu, P. A. Lahiji, *et al*., *Am. J. Physiol. Gastrointest. Liver Physiol.*, **291**, No. 2, G355-G363 (2006).
11. H. Kono, H. Fujii, Y. Hirai, *et al*., *J. Leukoc. Biol*., **79**, No. 4, 809-817 (2006).
12. T. A. Korolenko, I. A. Goncharova, L. I. Anterejkina, *et al*., *Alaska Med. J*., **49**, No. 2, 76-78 (2007).
13. M. McMillian, A. Y. Nie, B. Parker, *et al*., *Biochem. Pharmacol*., **67**, No. 11, 2141-2165 (2004).
14. M. Onda, M. Willingham, Q. C. Wang, *et al*., *J. Immunol*., **165**, No. 12, 7150-7156 (2000).
15. P. Schneider, T. A. Korolenko, and U. Busch, *Microsc. Res. Tech*., **36**, No. 4, 253-275 (1997).